Control of Particle Size and Morphology in Compatiblized Self-Catalyzed Co-Polyimide/SiO_2 Nanocomposites

[1,2] Farman Ali, [1,3]Shaukat Saeed*, Khaled M. Saoud and [2]Syed Sakhawat Shah
[1] *Department of Metallurgy and Materials Engineering (DMME), Pakistan Institute of Engineering and Applied Sciences (PIEAS), PO Nilore, Islamabad-45650, Pakistan.*
[2] *Department of Chemistry, Hazara University Mansehra, 21120, Pakistan.*
[3]*Liberal Arts and Science Program, Virginia Commonwealth University in Qatar, Doha, Qatar.*
saeedshaukat@yahoo.com, shaukat@pieas.edu.pk*

(Received on 15th March 2013, accepted in revised form 7th May 2014)

Summary: The size of the silica particles and morphology of hybrids were controlled in co-polyimide based hybrids through amino-silane functionalization of silica particles prepared *in situ* through a self-catalyzed sol-gel process using atmospheric moisture. The particles were generated using tetraethoxysilane in the uncompatiblized (UPISH) system whereas a mixture of 3-aminopropyltrietoxysilane and tetraethoxysilane was used in the compatiblized Co-PI/silica hybrid (CPISH) system. The properties of resulting hybrid films were measured by Fourier Transform Infrared Spectroscopy, Scanning Electron Microscopy, Thermogravimetirc Analysis, Dynamic Mechanical Analysis and Universal Testing Machine. FTIR results confirmed the formation of silica particles and Co-PI matrix. FE-SEM images revealed spherical silica particles with sharp boundaries in UPISH; whereas nano-sized coupled silica network structures with totally different morphologies were observed in CPISH system. The CPISH system exhibited better thermal stability, higher modulus and T_g values than UPISH system. The improvement in thermal and mechanical properties has been discussed with reference to morphological changes due to incorporation of 3-aminopropyltrietoxysilane in aerobic condition and in a self-catalyzed sol-gel process.

Key words: organic-inorganic hybrid; self-catalyzed sol-gel; polyimide; coupling agent; nanocomposites; thermal and mechanical properties.

Introduction

Simple blending of inorganic particles with organic polymers often improves the competence of the materials. However, organic-inorganic hybrids / nanocomposites show distinctive properties that conventional composites do not possess [1-6]. The advantages of organic polymer such as flexibility, elasticity, ductility, and process-ability and inorganic materials (inflexibility and high thermal stability) [7-11] are synergistically combined in the resulting materials. Silica is one of the inorganic components that have been explored extensively to improve the performance of organic polymers [12, 13]. Among the polymers, polyimides (PIs) are of special interest for their exceptional thermal and mechanical properties. Their outstanding characteristics, other than excellent thermal and mechanical properties, such as superior chemical resistance and low dielectric constant make them exceptional applicants as insulating materials for electronics, high-performance gas-separation membranes, high-temperature adhesives and coatings, and matrices for composites [14]. The many aspects of incorporation of nano-scale silica into polyimides, as source of further improving their mechanical properties and thermal stability, has been explored in recent past [11-15].

The method normally used for preparing PI/silica hybrids at mild conditions is to mix polyamic acid (PAA), a precursor for Polyimide, and alkoxysilane such as tetraethoxysilane (TEOS), followed by sol-gel reaction consist of acid catalyzed hydrolysis and polycondensation of alkoxysilane through addition of water. Desired particle size and structure is achieved by controlling the sol-gel process variables such as pH, concentration, water-to-alkoxysilane ratio, temperature, pressure, catalyst type, and solvent [16, 17]. Since water is a reactant in the sol-gel process, its concentration plays a vital role in the reaction kinetics and final structure of the material. It has been reported [18] that in a PI/silica system with excess water, the silica particles formed before the imidization of Polyamic acid and aggregated with the increase in temperature and degree of imidization. The additional water adversely effected the prevention of phase partition between PI and silica. Thus, by regulating the molar ratio of water to TEOS, the size and distribution of silica particles in PI matrix could be controlled leading to improvement in properties.

*To whom all correspondence should be addressed.

Another important factor that has a positive effect on thermal and mechanical properties is the improvement in interfacial bonding concerning organic and inorganic phases. Efforts have been made to enhance interfacial adhesion and to restrain the phase separation. The incorporation of coupling agents such as aminophenyltrimethoxysilane, aminopropyltrimthoxysilane, phenyltriethoxysilane, methyltriethoxysilane, γ-glycidyloxypropyl trimethoxysilane, (aminoethylaminomethyl)-phenethyltrimethoxysilane and socyanatopropyl trimethoxysilane [19-26] had marked effects on the morphology of the hybrid materials and has in many cases improved their thermal, optical, mechanical and dielectric properties.

During this investigation, we intend to control the size of the silica particles and morphology of Co-PI/silica hybrid materials through aminosilane modification of silica particles prepared *in situ* over/via a self-catalyzed sol-gel process using atmospheric moisture. The self-catalyzed sol-gel procedure avoids negative effects of mineral acids normally used as catalyst. The phase separation is expected to be hindered significantly as two unique features are associated with this synthesis approach. Firstly, it uses carboxylic acid groups of PAA to perform self-catalyzed hydrolysis and condensation reactions. Secondly, water required for hydrolysis of TEOS is derived from environmental moisture as well as the water molecules liberated during imidization of PAA, which ensures controlled availability of water. The interfacial contact between the PI and silica is enhanced by employing 3-aminopropyltriethoxysilane (APTES) as coupling agent. The resulting hybrid films were found to possess excellent transparency, good thermal stability, and improved mechanical properties along with ease in synthesis process.

Characterization

Spectroscopic analyses of the hybrid films were done using Fourier Transform Infra-Red Spectroscopy. Attenuated Total Reflection (ATR) module was used to obtain spectra in the range of 4000 – 400 cm^{-1} using Nicolet 6700 FTIR spectrometer. Cryo-fractured cross-sections of the hybrid films were sputter coated with gold for 30 sec and were scanned using a FE-SEM (JEOL 1550). Dynamic mechanical analyses (DMA) were carried out on a Pyris Diamond DMA (Perkin Elmer, USA). The DMA tests were performed in tension mode under nitrogen flowing at a rate of 50 ml/min. The samples were subjected to sinusoidal amplitude of 15 µm at a fixed frequency of 1 Hz from room temperature to 500 °C at a heating rate of 5 °C/min. Thermal stability of these nanocomposites was investigated from decomposition contours measured by thermogravimetry (TG) using Pyris Diamond thermal analyzer (Perkin Elmer, USA). The TG experiments were performed from room temperature to 1000 ^{o}C at a heating rate of 10 °C/min under flowing air at a rate of 50 ml/min. The mechanical properties of hybrid films were measured on a universal testing machine (UTM), M350/500 (Testrometric, UK) with a crosshead speed of 5 mm/min at room temperature using a load cell of 1 KN capacity.

Results and Discussion

Spectroscopic Analysis

ATR-FTIR spectroscopy was used to characterize the chemical structure of UPISH and CPISH films containing various amounts of silica. 'Fig. 1a and 1b shows the ATR spectra of UPISH and CPISH systems, respectively in 2000 – 500 cm^{-1} range.' Spectroscopic measurements were carried out on hybrids containing 10, 20 and 25 wt% silica to confirm the imidization of PI and formation of silica linkage in each hybrid system. The characteristic bands of imide group appear at 1777 cm^{-1} (imide C=O asymmetric stretching), 1727 cm^{-1} (imide C=O symmetric stretching), 1372 cm^{-1} (C–N stretching), and 726 cm^{-1} (imide ring deformation) [15, 27]. The presence of characteristic imide bands and absence of amide bands at 1657 cm^{-1} (C=O, amide I) and 1539 cm^{-1} (C–NH, amide II) endorse that the imidization was complete in all hybrid films. All the spectra show absorption bands at 1085 cm^{-1} that corresponds to ≷Si–O–Si≷ bonds stretching [27-29]. The results indicate that a three-dimensional silica network was formed during the thermal treatment of these hybrid materials.

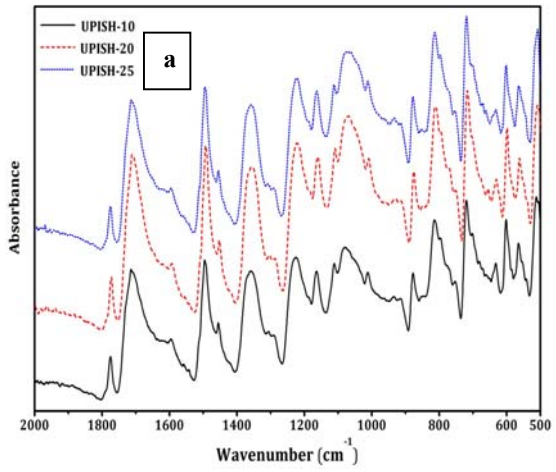

Fig. 1: (a): IR spectra of UPISH.

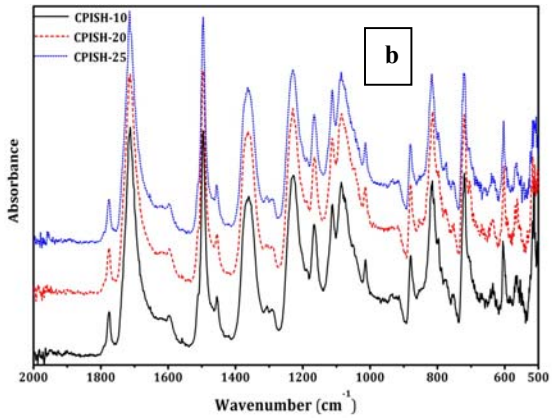

Fig. 1: (b): IR spectra of: CPISH films.

The difference between the IR spectra of UPISH and CPISH is the nature of silica network shaped in two types of hybrids. It is important to note from Fig. 1(a) that in UPISH, the size of the band around 1000-1100 cm^{-1} for corresponding silica loading is much more as compared to CPISH Fig. 1(b), the broad band may be due to the dissimilar nature of silica groups [30]. Similarly it can also be seen that the height of the CPISH bands is more as related to UPISH. The spectra in the range from 2000-4000 cm^{-1}usually contains absorption band centered on 3490 cm^{-1} due to the joined effect of C-OH bond stretching and uncondensed silanols (Si-OH) created as a result of hydrolysis of TEOS.

Microscopic Analysis

Most of the vital properties of composite materials are dependent on the degree of bonding between the two phases, surface area of the dispersed phase, and geometry of the reinforcing phase. Microscopic measurements were performed to explore the effect of silica particles generated through self-catalyzed sol-gel process on nature, size, and microstructure of the resulting composite materials in both uncoupled and coupled PI/silica hybrid systems. Fig. 2 shows FE-SEM micrographs of the brittle fractured surfaces of the samples containing 10 and 25 wt% silica in the two hybrid systems. The diameter of the particles in the UPISH is around 200 nm for UPISH-10 (Fig. 2(a)) and 4 µm for UPISH-25 (Fig. 2(b)) indicating an increase in particle size on increasing silica content. It is evident from the micrographs (Fig. 2 (a and b)) that the particles are spherical in shape with sharp boundaries, suggesting absence of chemical interaction between the two phases. To explore the effect of the coupling agent (APTES) and controlled availability of water on microstructure of the resulting hybrid materials, the samples of CPISH with similar silica content, i.e. 10 and 25wt%, were subjected to FE-SEM analysis. The micrographs of CPISH system are shown in Fig. 2(c and d). The size of PI-coated silica particles is in the range of 80 – 250 nm. The particles have diffused boundaries that suggest existence of covalent linkages between the inorganic particles and the organic matrix as has been reported earlier [29]. The observed reduction in size of silica particles and their polymer embedded morphology points toward the strong role of APTES along with synergistic effect of sol-gel reaction specific conditions in controlling the microstructure. The microstructural details suggest that CPISH system represents a true hybrid material of class-II type, where the two phases are chemically linked together [31]. Comparison of micrographs (Fig. 2) clearly indicates that addition of APTES produced a narrow but uniform size distribution and also significantly reduced the particle size. This reduction enhanced the compatibility between PI and silica due to enormous increase in interfacial area.

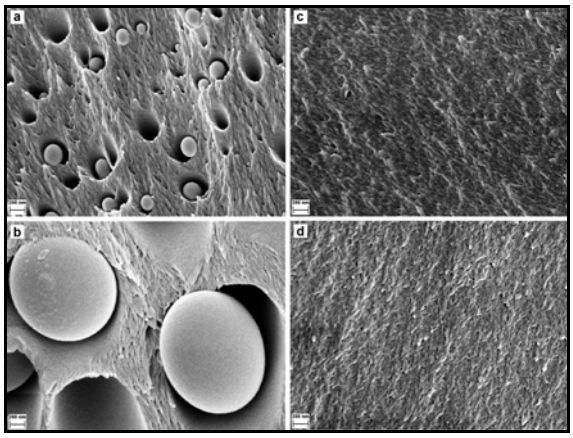

Fig. 2: SEM images of: (a) UPISH-10 and (b) UPISH- 25 indicating increase spherical silica particles with clear sharp boundaries; (c) CPISH-10 and (d) CPISH-25 revealing nano-sized silica particles with co-continuous morphology.

Dynamic Thermo-Mechanical Analysis

Temperature variations of the ratio of loss modulus to storage modulus (tan δ) for the pristine Co-PI, UPISH, and CPISH films are shown in Fig. 3. The tan δ values remain below ~0.025 up to around 280 °C, rise to maximum values of ~0.23 at around 395 °C for UPISH (Fig. 3(a)) and ~0.18 at around 400 °C for CPISH (Fig. 3(b)), and then fall again upon further increase in temperature. This abrupt rise in tan δ value is related with the onset of short-range

segmental motions known as α-relaxation or glass transition and the temperature corresponding to this phenomenon is called the glass-transition temperature (T_g). The T_g for Co-PI, UPISH-10, UPISH-25, CPISH-10, and CPISH-25 films appears at 385 °C, 396 °C, 398 °C, 402 °C, and 406 °C, respectively. It is evident that T_gs of all the hybrid films are higher than the pristine Co-PI. With increase in silica content, the tan δ trace after the onset of segmental motions spans over broader temperature range. The observed increase for CPISH system is attributed to a significant reduction in the particle size and enhanced interaction between organic and inorganic phases that restricted the segmental movement of PI chains**.**

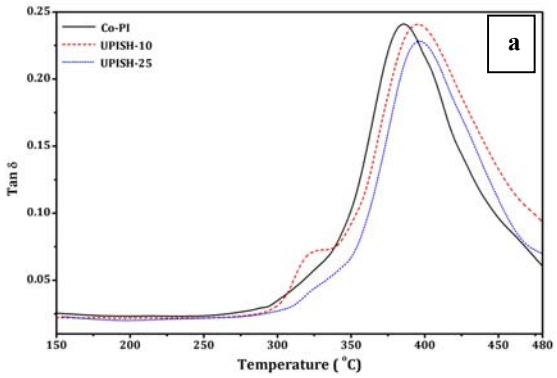

Fig. 3: (a): Variation of tan δ with temperature for: UPISH.

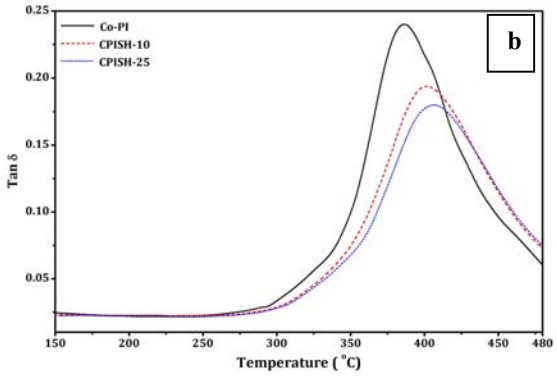

Fig. 3: (b): Variation of tan δ with temperature for CPISH films.

Mechanical properties

Mechanical properties are important for investigating effects of the structure of the reinforcing phase and the level of its interaction with the matrix phase on bulk properties of the composite material, defining its suitability for a specific application. Tensile properties of the UPISH and CPISH films were studied using Universal Testing Machine (UTM). The tensile stress-strain curves, fracture strength versus silica content, and Young's modulus versus silica content are shown in Fig. 4-6, respectively.

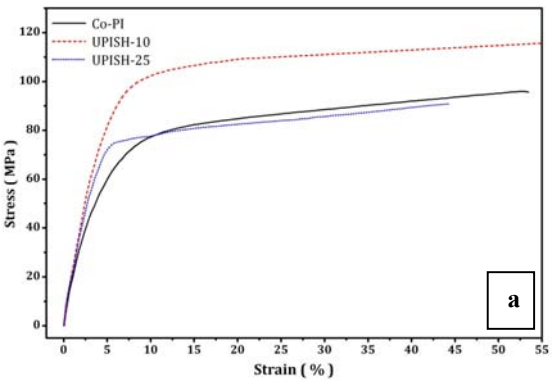

Fig. 4: (a): Stress-strain relationship for: (a) UPISH.

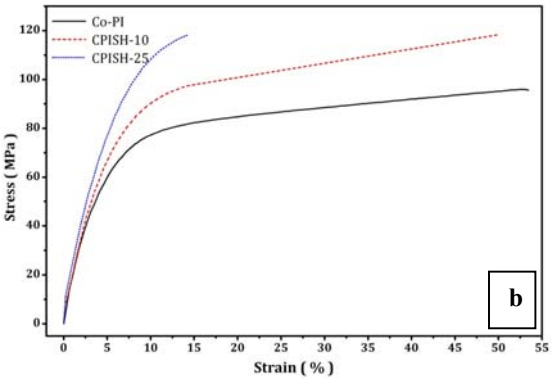

Fig. 4: (b): Stress-strain relationship for CPISH systems.

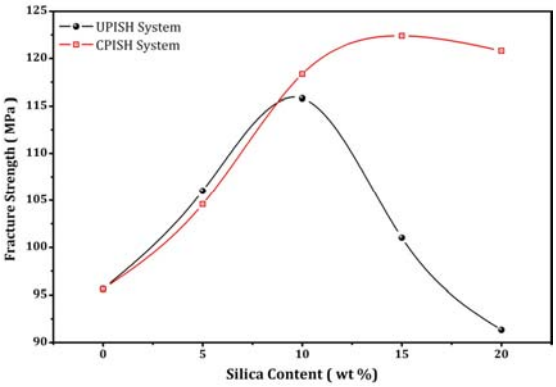

Fig. 5: Effect of silica content on fracture strength of UPISH and CPISH films.

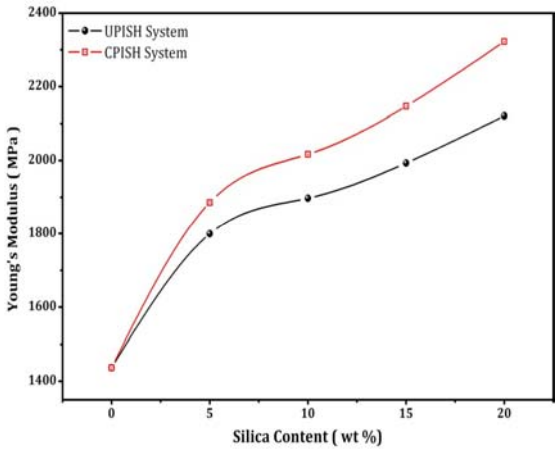

Fig. 6: Effect of silica content on Young's modulus of both UPISH and CPISH films.

In case of UPISH, hybrid film with 10 wt% silica content shows (Fig. 4(a)) the highest value of tensile strength. It can be observed that further silica loading decreases the tensile strength. The micro-structural details revealed by FE-SEM, where significant increase in size of silica particles with increase in silica content was noted in case of UPISH system, explains why the film with lower silica content fractured at higher stress than that with higher silica content. For a specific ceramic particles loading, the smaller sized particles accumulatively have larger surface area that, on application of the external load, may results in greater interaction with the organic matrix. In case of UPISH-10 film, enhanced interaction due to smaller size and uniform distribution of particles seems responsible for its improved mechanical strength. For the composition with higher silica content, the silica has agglomerated to larger particle sizes [12] leading to phase separation and therefore, its mechanical strength is decreased. Contrarily, the CPISH system shows a gradual increase in the tensile strength up to 20 wt% silica content.

The fracture strength values for each composition of UPISH and CPISH systems have been presented in Fig. 5. The maximum fracture strength observed in UPISH system is 111.8 MPa, whereas it is 122.8 MPa for CPISH system. The higher fracture strength for CPISH system is attributed to the fact that APTES not only provided chemical linkage between the two phases [6], but also led to the formation of nanometer sized particles under specific sol-gel reaction conditions. These factors contributed to efficient transfer of external mechanical stresses from organic matrix to the inorganic silica network. Thus the presence of coupling agent enhanced the interfacial interaction and also increased the efficiency of the hybrid material in transfer of stress from matrix to the reinforcing agent.

The variation of Young's modulus with silica content determined from the slope of the linear elastic region is shown in Fig. 6. A gradual increase in the value of Young's modulus with increase in silica content is evident however; a larger change is experienced in CPISH than in UPISH system. Keeping in view the morphology revealed by SEM, the existence of both chemical and physical interactions between the two phases in CPISH system is imperative that resulted in higher values of modulus; whereas only physical interactions are expected in case of UPISH system.

Thermogravimetirc Analysis (TGA)

The thermal stability of the hybrid films was investigated using TGA. The thermal curves depicted in Fig. 7 show that UPISH films are fairly stable up to 500 °C whereas the CPISH films resist degradation up to 550 °C. It is evident from the thermal curves that in both systems, massive degradation processes start beyond above mentioned temperatures that continue up to 710 °C for UPISH and 740 °C for CPISH systems and finally stabilize at a residual weight that approximately corresponds to added silica content. The improved thermal stability with increase in silica content, especially in CPISH films, may be due to the formation of char that act as protective layer and reduces the availability of oxygen for thermo-oxidative degradation.

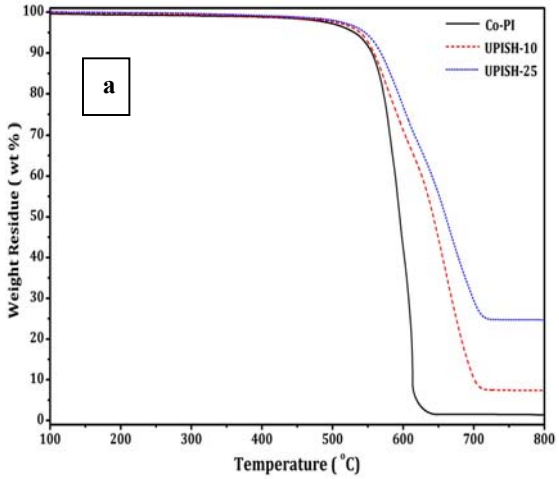

Fig. 7: (a): Thermal curves for: (a) UPISH.

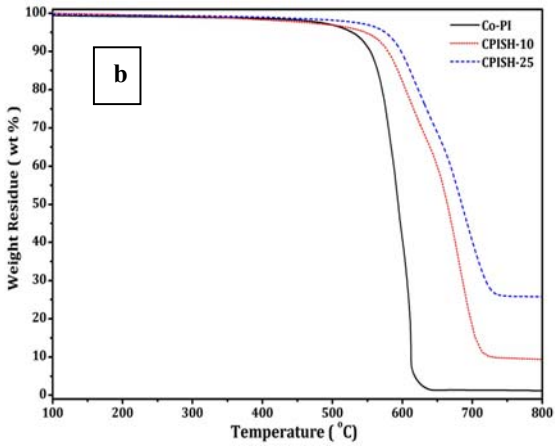

Fig. 7: (b): Thermal curves for CPISH systems.

Experimental

Materials

High purity chemicals [4, 4′-oxydianiline (ODA) 99.9%, Fluka; p-phenylenedianiline (p-PDA) 99.9%, Acros; pyromellitic dianhydride (PMDA) 99.2%, Aldrich; tetraethoxysilane (TEOS) 99.6%, Acros; 3-aminopropyltriehtoxysilane (APTES) 99%, Aldrich; and dimethylacetamide (DMAc) 99.8% (water content < 0.005%), Aldrich] were used as received.

Preparation of Co-polyamic acid

A mixture of diamines, ODA and p-PDA in 9:1 molar ratio, was charged in a two-neck flask fitted with a mechanical stirrer and was dissolved in DMAc. Stoichiometric amount of PMDA was added to the diamines solution and was stirred for 12 h to ensure the completion of reaction between diamines and dianhydride to form random Co-PAA. DMAc was added from time to time to facilitate stirring. Finally, a 10 wt% Co-PAA solution was obtained. The above reaction was carried out under anhydrous conditions maintained in a glove box. The reaction scheme for the synthesis of Co-PAA and Co-PI is shown in Fig. 8.

Preparation of uncoupled PI/silica hybrids (UPISH)

A 40 wt% TEOS solution in DMAc was prepared and calculated amounts from this stock solution were added to Co-PAA solution to prepare the final materials having 5 – 25 wt% silica content. For this addition the reaction flasks were shifted to open atmosphere, it was presumed that along with the water released during PAA condensation, solution would absorb some moisture from the surrounding atmosphere that would be utilized for hydrolysis of TEOS. The resulting solutions were vigorously stirred for 30 min at room temperature to ensure uniform distribution of TEOS in Co-PAA solution. The polymer solutions were stirred for 6 hours at 60 ^{o}C to carry out hydrolysis and condensation reactions. The contents were then poured in Teflon Petri dishes and converted to self-standing solid films by heating at 70 ^{o}C for 12 hours. Successive heating of these films at 100, 200, and 300 ^{o}C for 1 hours each resulted in PI/silica hybrid films. A compositions of PI/silica hybrids are given in Table-1.

Table-1: Composition of co-polyimide (Co-PI), uncoupled PI/silica hybrid (UPISH), and coupled PI/silica hybrid (CPISH) films

Material	ODA : *p*-PDA : PMDA (molar ratio)	TEOS : APTES (molar ratio)	Silica (Wt %)
Co-PI	9 : 1 : 10	0 : 0	0
UPISH-5	9 : 1 : 10	19 : 0	5
UPISH-10	9 : 1 : 10	19 : 0	10
UPISH-15	9 : 1 : 10	19 : 0	15
UPISH-20	9 : 1 : 10	19 : 0	20
UPISH-25	9 : 1 : 10	19 : 0	25
CPISH-5	9 : 1 : 10	19 : 1	5
CPISH-10	9 : 1 : 10	19 : 1	10
CPISH-15	9 : 1 : 10	19 : 1	15
CPISH-20	9 : 1 : 10	19 : 1	20
CPISH-25	9 : 1 : 10	19 : 1	25

Preparation of coupled PI/silica hybrids (CPISH)

TEOS and APTES in 19:1 molar ratio were mixed in DMAc to prepare a 40 wt% stock solution. Pre-calculated amounts of this solution were then added to Co-PAA solution to prepare final materials containing 5 – 25 wt% silica (Table-1). Each solution was stirred for 30 min at room temperature to ensure uniform mixing of the silanes solution in Co-PAA. The resulting mixture was further stirred for 6 hours at 60 ^{o}C. The drying and thermal imidization was carried out in the same way as described under Section 4.3.

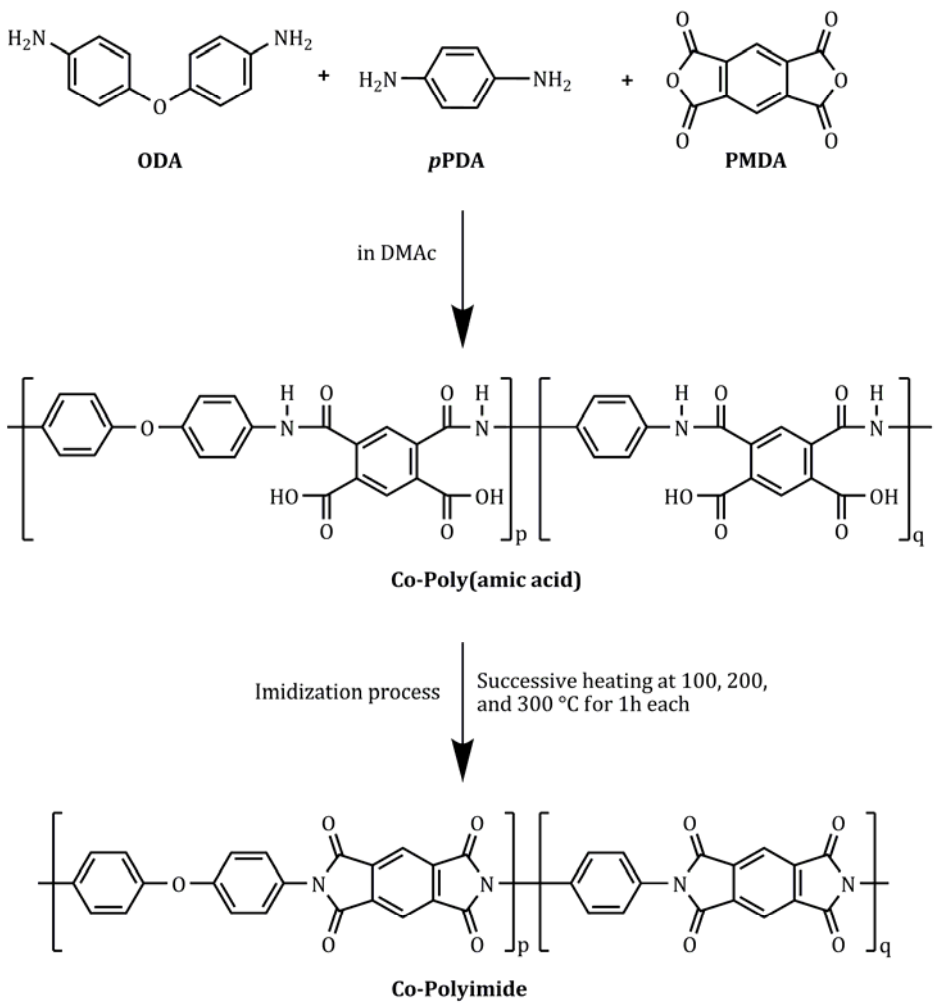

Fig. 8: Reaction scheme for the synthesis of polyimide.

Conclusion

UPISH and CPISH systems containing 0 to 25 wt% silica were successfully synthesized in aerobic condition to carry out sol-gel hydrolysis and condensation reactions. The FTIR analysis confirmed the formation of polyimide as well as the generation of silica network. The SEM micrograph revealed an appreciable reduction in size of the silica particles due to incorporation of the coupling agent. The APTES produced covalent linkages between the inorganic particles and the polymer matrix. The CPISH system was found to have higher Tg values, enhanced mechanical strength, and high values of Young's moduli compared to pristine Co-PI and UPISH system. The improved thermal stability of hybrid films, especially of CPISH system, may be due to formation of a protective layer that restricted diffusion of oxygen in PI/silica network.

References

1. M. Nandi, J. A. Conklin, L. Salvati and A. Sen, *Chemistry of Materials,* **3**, 201 (1991).
2. Q. Hu and E. Marand, *Polymer,* **40**, 4833(1999).
3. M. Khalil, S. Saeed and Z. Ahmad, *Journal of Macromolecular Science part* A, **44**, 55 (2007).
4. J. Habsuda, G. P. Simon, Y. B. Cheng, D. G. Hewitt, D. R. Diggins and H. Toh, *Polymer,* **43**, 4627 (2002).
5. J. N. Hay and H. M. Raval, *Chemistry of Materials,* **13**, 3396 (2001).
6. Z. Ahmad and J. E. Mark, *Chemistry of Materials,* **13**, 3320 (2001).
7. W. C. Chen, L. H. Lee, B. F. Chen and C. T Yen, *Journal of Material Chemistry,* **12**, 3644 (2002).
8. L. H. Lee and W. C. Chen, *Chemistry of Materials,* **13**, 1137 (2001).

9. C. C. Chang and W.C. Chen, *Journal of Polymer Science Part* A, **39**, 3419 (2001).
10. L. Zhili, H. Wei, K. Dimitry, C. M. Jose, B. Zijp and C. Peter, *Polymer,* **47**, 1150 (2006).
11. T. Akhter, S. Saeed, H. M. Siddiqi, O. O. Park, *Journal of Polymers for Advanced Technologies,* **24,** 407 (2013).
12. S. Wang, Z. Ahmad and J. E. Mark, *Chemistry of Materials,* **6**, 943 (1994).
13. L. Mascia and A. Kioul, *Polymer,* **36**, 3649 (1995).
14. C. Xenopoulos, L. Mascia and S. J. Shaw, *Chemistry of Materials,* **12**, 213 (2002).
15. C. C. Chang and W. C. Chen, *Chemistry of Materials,* **14**, 4242 (2002).
16. S. Yano, K. Iwata and K. Kurita, *Material Science Engineering,* **C 6**, 75 (1998).
17. S. Wang, Z. Ahmad and J. E. Mark, *Chemistry of Materials,* **6**, 943 (1994).
18. A. Kioul and L. Mascia, *Non-Crystalline Solids,* **175**, 169 (1994).
19. Y. Iyoku, M. Kakimoto and Y. Imai, *High Performance Polymer,* **6**, 43 (1994).
20. C. Xenopoulos, L. Mascia and S. J. Shaw, *Material Science Engineering,* **6**, 99 (1998).
21. J. Schrotter, M. Smain and C. Guizard, *Advance Polymer Science,* **61**, 2137 (1996).
22. L. Beecrft, N. A. Johnen and C. K. Ober, *Polymer for Advance Technology,* **8**, 289 (1997).
23. Z. Z. Kang, Y. Yang, J. Yin and Qi. Neng, *Applied Polymer Science,* **73**, 2977 (1999).
24. A. Arbash, F. A. Sagheer, M. Ali A. A and Z. Ahmad, *International Journal of Polymer Materials,* **55**, 103 (2006).
25. W. Y. Wen, Y. Cheng-Tyng and C. W. Chang, *Polymer,* **46**, 6959 (2005).
26. T. Seckin, A. Gultekand and S. Koytepe, *Turkish Journal of Chemistry,* **29**, 49 (2005).
27. M. Simionescu, M. Marcu and M. Cazacu, *European Polymer Journal,* **39**, 777 (2003).
28. C. Kaynak, C. Celikbielk and G. Akovali, *European Polymer Journal,* **39**, 1125 (2003).
29. S. Saeed, M. Khalil and Z. Ahmad, *Journal of Macromolecular Science part* A, **46**, 152 (2009).
30. M. Khalil, S. Saeed and Z. Ahmad, *Journal of Applied Polymer Science*, **107**, 1257 (2008).
31. G. Kickelbick, Introduction to hybrid materials, in Hybrid Materials, Synthesis, Characterization and Applications, Wiley-VCH Verlag GmbH & Co. KGaA, Weinheim, ISBN: 978-3-527-312999-3, pp. 1-48 (2007).